

QUANTITATIVE REAL-TIME PULSED SCHLIEREN IMAGING OF ULTRASONIC WAVES

A. HANAFY* and C. I. ZANELLI†

*Acuson Corporation, Mountain View, CA 94039, †Intec Research Co., Sunnyvale, CA 94089.

ABSTRACT

A pulsed Schlieren system based on Raman-Nath scattering by ultrasonic waves in water is described. High powered, monochromatic infrared pulsed light is used in conjunction with axial optics and a video camera to visualize the acoustic field. Projection beam profiles in any plane parallel or orthogonal to the direction of acoustic propagation are demonstrated. Controlled delay between acoustic pulse and light flash allows scrutinizing wave fronts at variable delay after launching. The method is applicable with reasonable repetition rates to broadband acoustic pulses with intensities in the medical diagnostic range. Quantification of the pressure density by analysis of the video signal is shown using a single-point calibration against a total acoustic power measurement by the force balance method, without a priori assumptions about the beam structure.

INTRODUCTION

Ultrasound equipment for medical and other applications requires measuring their acoustic output to insure safe and optimal performance. This article describes a method to both visualize and measure beam parameters without disturbing the sound beam.

Schlieren is an imaging technique based on the Raman-Nath¹ theory in which the acoustic beam is treated as a phase grating. Appropriate optics allows forming a near-field image of the phase grating onto film or a video array. Strobbing the light source at a fixed delay after the launch of ultrasound pulses allows the image of a wave packet to appear stationary for viewing on a TV monitor, or photographic recording.

Video images are particularly useful in visualizing the whole field at once, whereas a hydrophone survey requires knowing the general area and time in which one is to find the acoustic wave. The video signal has been previously used directly to measure the radiance⁴,

and here we report a means to use the video signal to measure the acoustic intensity integrated over the acousto-optic interaction path. Integration over time yields, then, the total acoustic power.

Correlation between collected light intensity and acoustic radiation pressure allows further quantitative analysis of the image captured with a video frame grabber.

Raman-Nath scattering

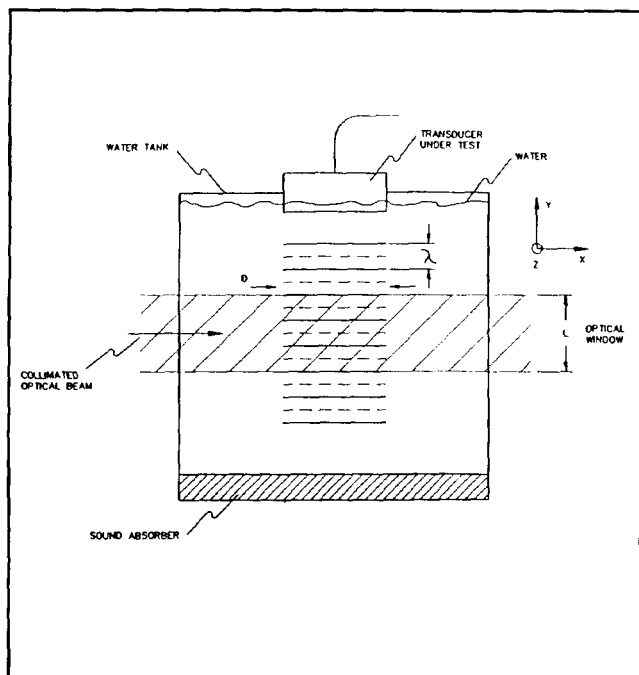


Figure 1. Geometry for Schlieren scattering.

Consider the scattering condition depicted in figure 1. If ultrasound and optical parameters are within the Raman-Nath regime, i.e.

$$D k_a^2 \ll k_0 \quad (1)$$

(where D is a measure of the beam width, k_a the acoustic wave number, and k_0 the optical wave number). The radiance in each diffracted order provides a measure of the acoustic intensity integrated over the interaction length,

$$I_n = J_n^2(\nu) \quad (2)$$

where J_n is the n-th order Bessel function. ν is the integrated optical phase shift along the interaction length, also called the Raman-Nath parameter:

$$\nu(y,z) = k_{e0} p_{op} \int P_i(x,z) \sin(\omega_a t + k_a y + \phi_a(x,z)) dx \quad (3)$$

where k_{e0} is the electromagnetic wave number in vacuum, p_{op} is the piezo-optic constant⁶, P_i is the acoustic pressure, and $\phi(x,z)$ is a phase term responsible for acoustic focusing.

For simplicity, consider an unfocused beam, i.e. $\phi \ll 2\pi$ throughout the area of integration. Then the integrated phase shift ν reduces to the line integral of the pressure, modulated in time at the frequency ω_a ,

$$\nu(y,z) = A \sin(\omega_a t + k_a y) I_p(z) \quad (4)$$

where

$$I_p(z) = \int P_i(x,z) dx \quad (5)$$

It has been shown⁷ that if the zero-th order (J_0) is suppressed but the positive and negative higher orders are preserved, the time dependency cancels out. Clearly the zero-th order can only be suppressed if some of the higher orders --particularly the first-- are reduced too (as the Bessel functions overlap). However, the use of a "dot" stop that encompasses most of the zero-th order, yet allows both negative and positive diffraction terms to be collected and added (in phase) at the focal plane presents a significant advantage over the knife-edge method. Then, the collected light intensity coming from a point (y,z) in the image plane, to first approximation, is

$$I_{coll}(y,z) \approx J_1^2[A(y) I_p(z)] \quad (6)$$

Where $A(y)$ contains the y-dependency. Now, for the Raman-Nath regime $A(y) \times I_p(z) \ll 1$, so equation (6) can be approximated further to

$$I_{coll}(y,z) \approx \text{Constant} \times A^2(y) I_p^2(z) \quad (7)$$

and an integration along the z axis is proportional to the total integral of P_i^2 , i.e. to the total acoustic power (in the far field) transmitted across the $y=y_0$ plane:

$$TAP(y_0) = \text{Constant} \times \int I_{coll}(y_0,z) dz \quad (8)$$

It should be noted that, for a non-dispersive medium, the y dependency of this integral vanishes due to energy conservation.

METHODS

Optics

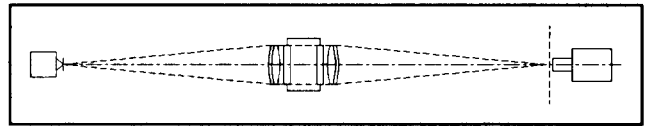


Figure 2. Optical layout of lens-based Schlieren system.

A schematic diagram of a lens-based Schlieren optical system is shown in figure 2 above. The system requires an intense point source of light, such as a laser or an arc lamp, to produce uniform illumination of the object to be studied. The object itself should be reasonably transparent so phase perturbation of the illumination beam is the dominating feature in the image. Direct light from the source is blocked at the zero-th order stop in the optical axis, and then re-imaging optics are used to develop an image of the relatively weak light levels scattered by the phase perturbations. In the absence of direct light from the source, the normally invisible phase perturbations are changed into visible intensity variations, rendering an "ordinary" looking image of the object. The usefulness of such phase images is usually greatest when the phase perturbations produced by the object are less than a few wavelengths of the illumination light - a condition satisfied quite well by the pressure levels produced from medical diagnostic ultrasound transducers operating in a water tank.

Although the major conceptual difference between a Schlieren optical system and a "standard" optical imaging system is the use of a point illumination source combined with blocking of the direct (zero-th order) light, the ability of the Schlieren system to render visible small phase perturbations in light passing through the object makes it necessary to use optics of the highest quality. Normally invisible flaws and bubbles in the optical components themselves are also made visible with the system.

As discussed above, in order to achieve a relatively flat frequency response it is essential to block *only* the zero-th diffraction order. The conventional approach of using a sharp knife edge deprives the image plane of one complex conjugate for each diffraction order, resulting in the familiar fringes³. These fringes do not correspond to acoustic intensity but to interference between diffraction orders, without the benefit of phase cancellation by the presence of the symmetrical diffraction beam.

Given that the light intensity at the image (and thus the amplitude of the video signal) is proportional to the acoustic intensity, the dynamic range in determining intensity levels is only half the dynamic range of the sensing device. This effect is the leading cause for the dynamic range limitation usually encountered in Schlieren systems.

Electronics

Key in visualizing acoustic pulses is variable-delay circuitry that is triggered synchronously with the acoustic pulse, and provides a trigger signal for the light source after a controlled delay. In our case, a dual-purpose circuit was designed to either have a manually controlled delay or a delay which increases in time, allowing a quite didactic display of the waveform evolution away from the transducer.

The light source employed for imaging is a laser diode transmitting at 810 nm, with a peak power of 100 W and light pulses 200 to 500 ns wide. The driving pulser is limited to a maximum repetition rate to insure diode longevity.

Finally, video circuitry allows observing a given segment of a video line on an oscilloscope. The use of a digitizing oscilloscope presents advantages as averaging increases signal-to-noise ratio, and data can be extracted for further processing, such as integration.

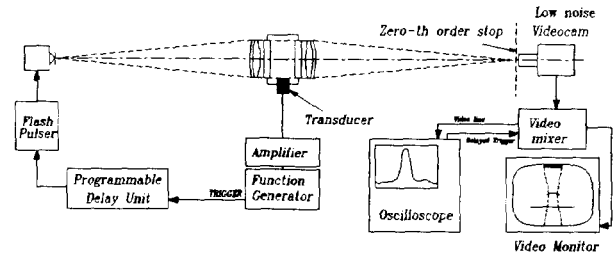


Figure 3. Complete layout of Schlieren system described in the text.

A schematic diagram for the whole system, including electronics, is shown in figure 3.

RESULTS

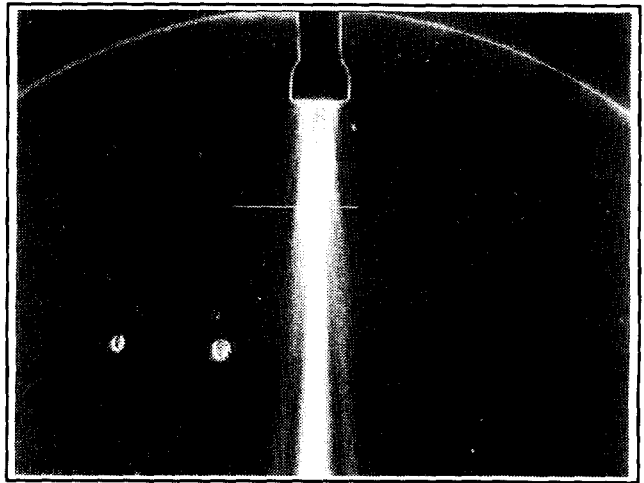


Figure 4a. Video image obtained with a CW beam at 2 MHz.

A video image obtained with the system described above is shown in figure 4a, and the corresponding video line amplitude is plotted in figure 4b. The vertical axis in figure 4b (mV) is calibrated with a single point to correspond to intensity line integral defined by equation (7).

Figure 5 depicts the correlation found between the amplitude of the video signal (RS-170) and the intensity line integral. The deviation past 500 mV was traced to saturation of the video array.

Integrating the video line and accounting for the video image scaling, the video amplitude (proportional to the

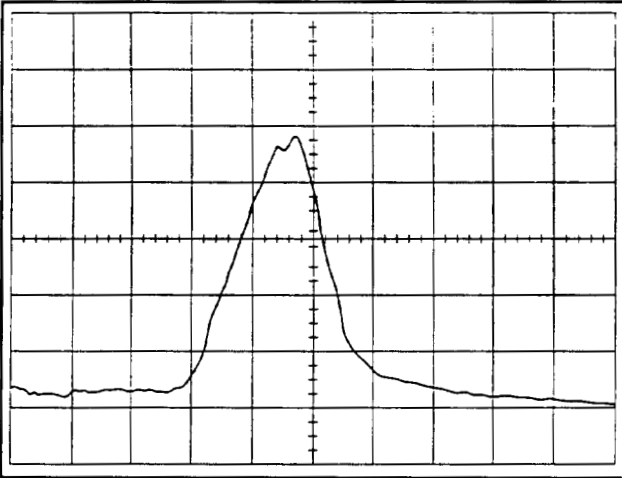


Figure 4b. Video line intensity from figure 4a.

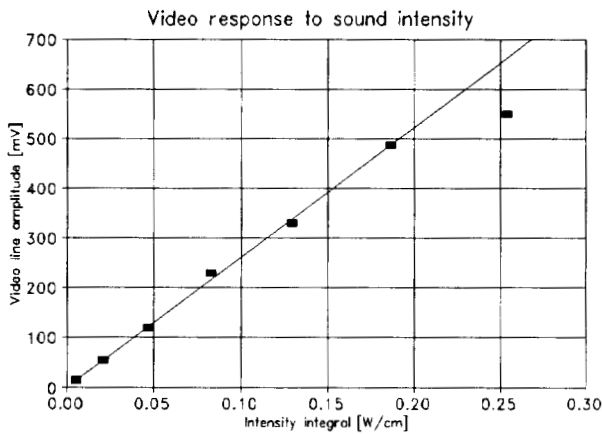


Figure 5. Video signal amplitude versus acoustic intensity line integral.

acoustic intensity line integral along x) integrated across the beam (z direction) yields the total acoustic power (TAP).

A comparison between TAP measured by these two independent means is shown in figure 6. A slight underestimation by the video method, attributed to detector saturation, is noticeable above 2.5 Watts. Detector saturation can be avoided by reducing the light source intensity, at the expense of increased noise.

An interesting application of the quantitative Schlieren technique is shown in figure 7, as the acoustic beam is oriented parallel to the video line.

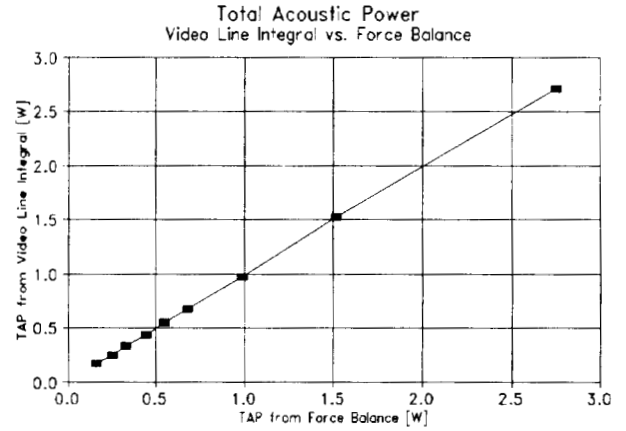


Figure 6. Acoustic power measured by independent means.

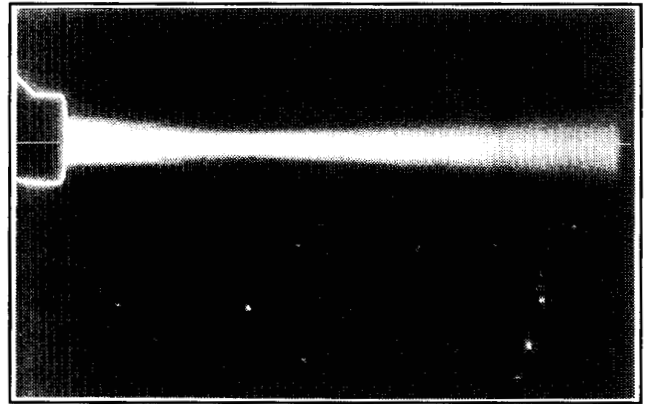


Figure 7. Acoustic beam along the video scan line.

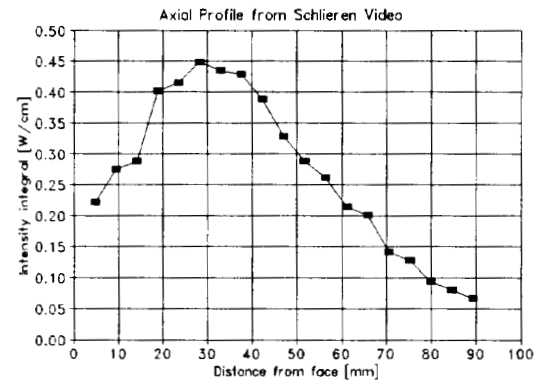


Figure 8. Axial beam profile, from figure 7.

Extraction of the video line intensity produces an axial beam profile in real time, as shown in figure 8.

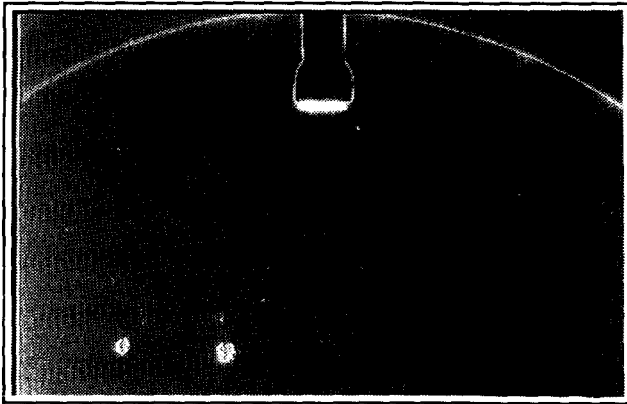


Figure 9

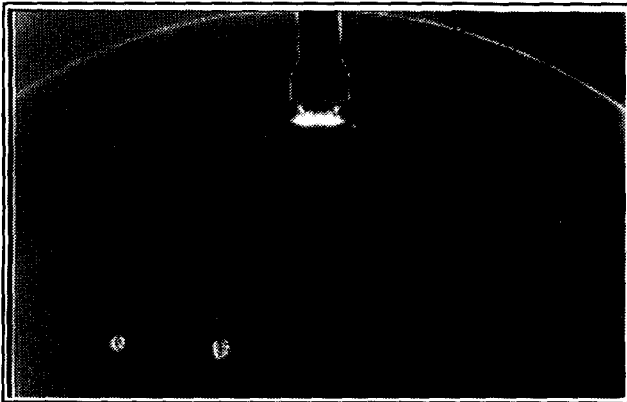


Figure 10

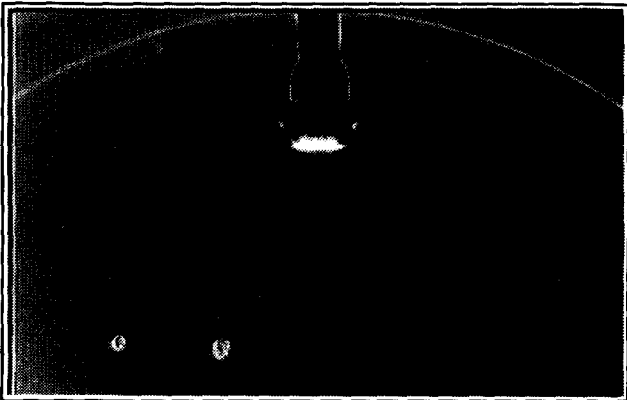


Figure 11

Figures 9 through 12 contain video images that illustrate some interesting effects such as sidelobe formation and near-field structure.

CONCLUSIONS

The described system is appropriate for imaging of pulsed or continuous wave ultrasound. The sensitivity is very high due to the high intensity light pulses that can be achieved with the laser diode source, and dynamic

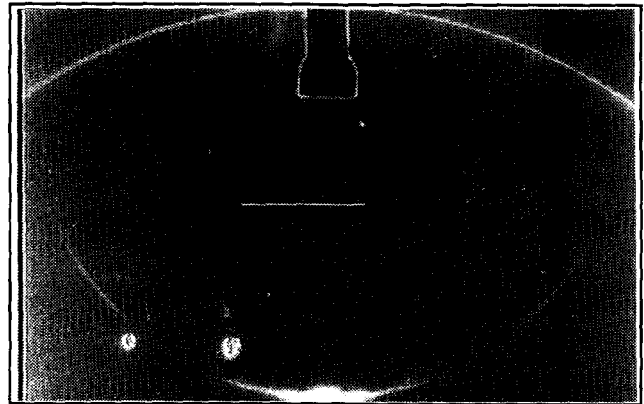


Figure 12

range is only limited by the imaging sensor. It is conceivable that, with integrating sensors, dynamic ranges of up to 50 dB are within reach.

For transducers designed for pulsed mode operation, this system allows power measurements at operating intensities in either single pulse or burst mode, thus avoiding the need for rf power amplifiers (except to calibrate) and without the risks associated with heating in CW mode.

ACKNOWLEDGEMENTS

The authors wish to thank Mr. Larry Bruno at Acuson for his support in assembling this system, and also to Acuson engineering services department for preparing the poster presentation that accompanied this paper.

REFERENCES

1. Raman, C.V. and Nath, N.S., The diffraction of light by high frequency ultrasonic waves. Proc. Indian Acad. Sci. II, 406 (1935).
2. Goodman, J., Introduction to Fourier Optics. McGraw Hill, New York (1968).
3. Hanafy, A. Ultrasonic Imaging 1, 295-302 (1979).
4. Hanafy, A. Ultrasonic Imaging 2, 122-134 (1980).
5. Haran, M.E., Cook, B.D. and Stewart, H.F. J. Acoust. Soc. Am. Vol. 57, No. 6, Part II (1975).
6. Riley, W.A. Jr., Love, L.A. and Griffith, D.W. J. Acoust. Soc. Am. Vol. 71, No. 5 (1982).
7. B.D. Cook, J. Acoust. Soc. Am 60, 95-99 (1976).

